Behavioral/Cognitive

Emotional Context Sculpts Action Goal Representations in the Lateral Frontal Pole

Regina C. Lapate,[1] Ian C. Ballard,[2] Marisa K. Heckner,[3] and Mark D'Esposito[2]
[1]Department of Psychological & Brain Sciences, University of California, Santa Barbara, Santa Barbara, California 93106, [2]Helen Wills Neuroscience Institute, University of California, Berkeley, Berkeley, California 94720, and [3]Institute of Neuroscience and Medicine, Research Centre Jülich, 52428 Jülich, Germany

Emotional states provide an ever-present source of contextual information that should inform behavioral goals. Despite the ubiquity of emotional signals in our environment, the neural mechanisms underlying their influence on goal-directed action remains unclear. Prior work suggests that the lateral frontal pole (FPl) is uniquely positioned to integrate affective information into cognitive control representations. We used pattern similarity analysis to examine the content of representations in FPl and interconnected mid-lateral prefrontal and amygdala circuitry. Healthy participants ($n = 37$; $n = 21$ females) were scanned while undergoing an event-related Affective Go/No-Go task, which requires goal-oriented action selection during emotional processing. We found that FPl contained conjunctive emotion–action goal representations that were related to successful cognitive control during emotional processing. These representations differed from conjunctive emotion–action goal representations found in the basolateral amygdala. While robust action goal representations were present in mid-lateral prefrontal cortex, they were not modulated by emotional valence. Finally, converging results from functional connectivity and multivoxel pattern analyses indicated that FPl emotional valence signals likely originated from interconnected subgenual anterior cingulate cortex (ACC) (BA25), which was in turn functionally coupled with the amygdala. Thus, our results identify a key pathway by which internal emotional states influence goal-directed behavior.

Key words: **cognitive control; emotion; emotion–cognition interactions; lateral frontal pole; prefrontal organization; representational similarity analysis**

Significance Statement

Optimal functioning in everyday life requires behavioral regulation that flexibly adapts to dynamically changing emotional states. However, precisely how emotional states influence goal-directed action remains unclear. Unveiling the neural architecture that supports emotion–goal integration is critical for our understanding of disorders such as psychopathy, which is characterized by deficits in incorporating emotional cues into goals, as well as mood and anxiety disorders, which are characterized by impaired goal-based emotion regulation. Our study identifies a key circuit through which emotional states influence goal-directed behavior. This circuitry comprised the lateral frontal pole (FPl), which represented integrated emotion–goal information, as well as interconnected amygdala and subgenual ACC, which conveyed emotional signals to FPl.

Introduction

Optimal functioning in everyday life requires behavioral control that is goal oriented yet flexible to dynamically changing contexts. One's emotional state—and the emotional states of others—are a primary source of such context. Emotional cues, such as others' facial expressions, often provoke automatic action tendencies, such as approach toward appetitive stimuli, and avoidance of aversive stimuli. These emotion-driven action tendencies can inform, amplify, or interfere with goal-directed behavior. For instance, receiving a welcoming smile in a new circle of neuroscientists potentiates the existing (approach-related) goal pursuit of sharing a collaborative research proposal (whereas a scorn would likely provoke the opposite reaction, hindering goal completion). Despite the ubiquity of emotional information in our

Received July 25, 2021; revised Dec. 13, 2021; accepted Dec. 14, 2021.

Author contributions: R.C.L., M.K.H., and M.D. designed research; R.C.L. and M.K.H. performed research; R.C.L. and I.C.B. contributed unpublished reagents/analytic tools; R.C.L. analyzed data; R.C.L., I.C.B., M.K.H., and M.D. wrote the paper.

This work was funded by National Institutes of Health Grants F32-MH-113347 (R.C.L.), F32-MH-119796 (I.C.B.), and MH-63901 (M.D.); National Science Foundation Award BCS-0821855 (M.D.); and the Wheeler Foundation. We thank Jeanette Mumford, Arielle Tambini, Jacob Miller, and Jingyi Wang for helpful discussions; Lennart Verhagen for access to the PFC consensus atlas; and Audrey Phan, Jenna Martin, and Jean Wu for assistance with data collection.

The authors declare no competing financial interests.

Correspondence should be addressed to Regina C. Lapate at lapate@ucsb.edu.

https://doi.org/10.1523/JNEUROSCI.1522-21.2021

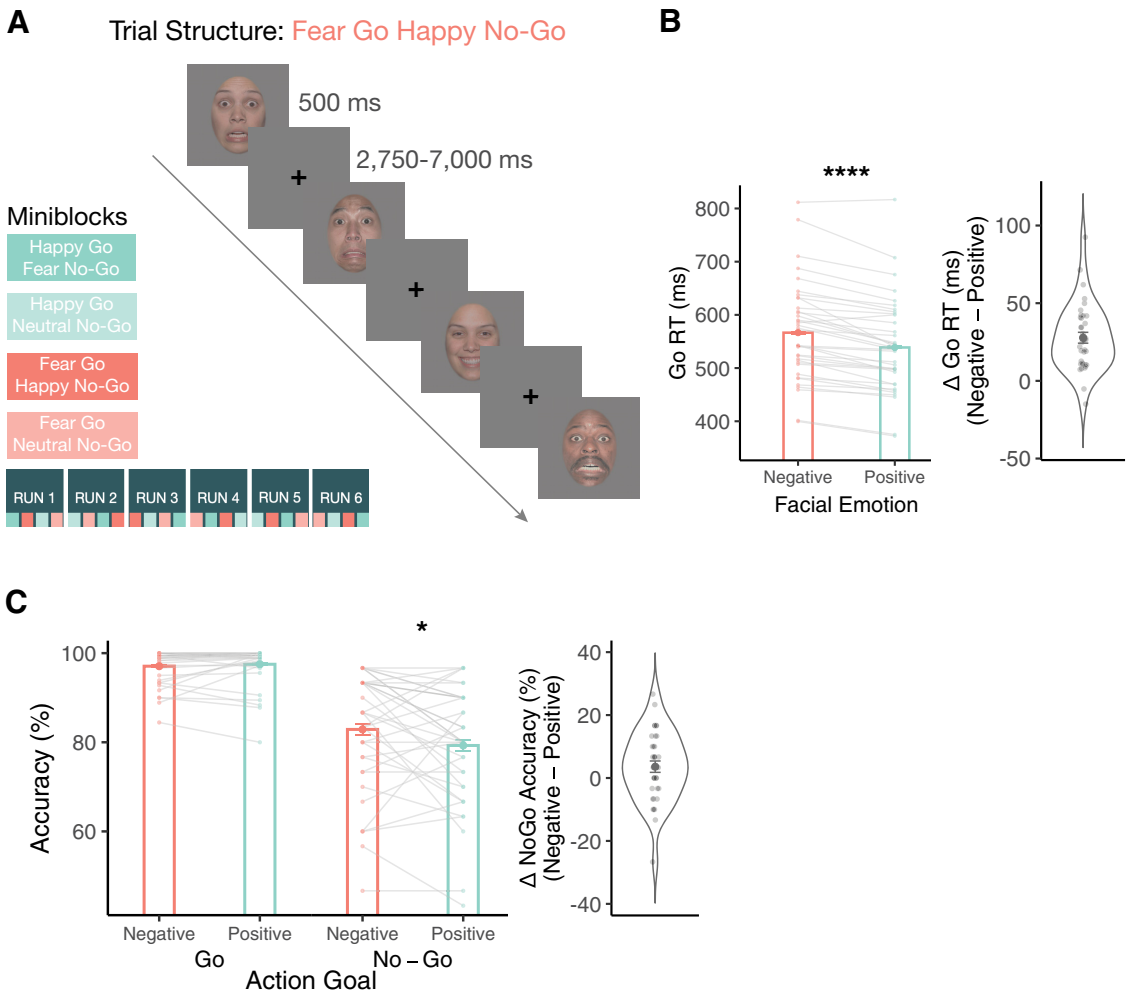

Figure 1. Emotional valence biases action. ***A***, The trial structure of the Affective Go/No-Go Task is shown. At the start of each condition miniblock ($n = 20$ trials), participants were asked to press a button (Go) in response to either happy or fearful faces, and to withhold responses (No-Go) following the presentation of nontarget emotional expressions (happy, fearful, or neutral faces). The experiment comprised a total of six fMRI scans, and each fMRI scanner run contained $n = 4$ miniblocks presented in counterbalanced order. ***B***, RT data for Go trials. Positive emotional valence (happy facial expressions) facilitates approach responses compared with negative valence (fearful expressions), reducing Go reaction times. The violin plot shows the distribution of the valence difference score in RTs (Negative – Positive). ***C***, Task accuracy data. Negative emotional valence facilitates avoidance responses, increasing accuracy for No-Go trials. The violin plot shows the distribution of the valence difference score in No-Go accuracy (Negative – Positive). *$p < 0.05$, ****$p < 0.0001$.

environment, the neural mechanisms underlying the potentiation (or interference) of goal-directed behavior by emotional signals remain underspecified.

Recent anatomic evidence suggests that the lateral frontopolar cortex may mediate the influence of emotion on goal-directed behavior. The lateral frontal pole (FPl) is ideally positioned to integrate and transmit information about internal states to the rest of lateral prefrontal cortex (LPFC). Unlike other LPFC regions, FPl receives projections from the amygdala via the ventral amygdalofugal pathway (Kamali et al., 2016; Folloni et al., 2019). Stronger structural connectivity of this pathway is associated with a stronger influence of emotion on action execution (Bramson et al., 2020). Disruption of FPl with transcranial magnetic stimulation amplifies the influence of emotional expressions on approach and avoidance behavior (Volman et al., 2011). Microstructural properties of the frontopolar cortex—including relatively low cell body density and reduced laminar differentiation, combined with increased dendritic length and spine number, compared with caudal and mid-lateral PFC regions—suggest that it has the highest level of information integration within the PFC (Jacobs et al., 2001; Badre and D'Esposito, 2009; Badre and Nee, 2018). However, because prior work has not used multivariate methods to examine FPl representations, it remains unclear whether FPl goal representations differ depending on ongoing emotional states (i.e., reflecting emotion-goal integration). Neural representations that integrate across distinct dimensions, such as goals and emotional states (also called conjunctive representations) have been postulated to be particularly advantageous for flexible and context-sensitive behavior, which is critical during emotional processing (Fusi et al., 2016; Badre et al., 2021).

To test whether FPl representations integrate across goals and emotional information and are associated with the influence of emotional signals on goal-directed behavior, we adapted a task that requires cognitive control during emotional processing, the Affective Go/No-Go (AGNG) task, for an event-related functional magnetic resonance imaging (fMRI) experiment. In the AGNG task, emotional valence ("Positive" vs "Negative," here happy and fearful faces) and goal (i.e., action goals: "Go" vs "No-Go") are manipulated orthogonally (Fig. 1*A*). Critically, emotion biases action goals depending on emotion–action congruency: in some trials, positive stimuli are Go targets (emotion–action congruent); in others, negative stimuli are Go targets (emotion–action incongruent), and vice versa. Positive stimuli typically

facilitate approach behavior [e.g., reducing Go reaction times (RTs)], whereas negative stimuli facilitate avoidance (e.g., increasing No-Go accuracy; Hare et al., 2005; Tottenham et al., 2011; Zhuang et al., 2021). Thus, Go RT and No-Go accuracy difference scores in the AGNG task provided indices of emotion-driven influence on action (i.e., affect-to-motor spillover).

We interrogated the content of neural representations in FPl and interconnected brain regions, including mid-LPFC (known to represent task goals; Waskom et al., 2014; Cole et al., 2016) and basolateral amygdala (BLA; known to support emotional valence encoding; Tye, 2018). To test whether emotion modulated action goal representations, we used pattern similarity analysis (Kriegeskorte and Kievit, 2013). Classifier decoding and functional connectivity analyses complemented pattern similarity analysis to further reveal the informational structure and behavioral correlates of emotion and action goal representations in FPl and interconnected circuitry. We hypothesized that FPl would represent integrated emotion and action goals; conversely, that basolateral amygdala and mid-LPFC would contain separate emotional valence and goal representations, respectively.

Materials and Methods

Participants

Forty participants were recruited from Berkeley, CA (mean age = 22.22 years; SD = 3.14; age range = 18–29 years; 24 female). Two subjects were excluded because of excessive motion (>3 mm), and one chose not to complete the study. Thus, the full sample analyzed here comprised 37 participants (mean age = 22.24 years; SD = 3.22; age range = 18–29 years; 21 female). All participants were healthy, with no self-reported history of neurologic or psychiatric disorders, and had normal or corrected-to-normal visual acuity. Written informed consent was obtained from each subject. Subjects were recruited at the University of California, Berkeley. All study procedures were approved by the UC Berkeley Committee for the Protection of Human Subjects. Participants were compensated monetarily for their participation.

Procedure

Overview

Participants underwent the AGNG in the MRI scanner as part of a longitudinal transcranial magnetic stimulation study on prefrontal mechanisms of emotion regulation. As part of this larger study, participants performed a resting-state and diffusion imaging scan (data not reported here). Following the informed consent procedure, participants practiced a few trials of the AGNG task before beginning the experiment. After ~40 min of fMRI data collection during the AGNG task, a high-resolution T1-weighted anatomic scan was obtained. At the end of the experiment, participants completed questionnaires (data not reported here).

Experimental design and statistical analysis

AGNG task. In the MRI scanner, participants completed the AGNG task. The task was composed of six functional runs (lasting ~7 min each). Each functional run contained four action goal + emotion target miniblocks: "Go Happy, No-Go Fear", "Go Fear, No-Go Happy", "Go Happy, No-Go Neutral", and "Go Fear, No-Go Neutral." Each miniblock contained 20 trials, 75% (15 of 20) of which were Go trials, and 25% (5 of 20) were No-Go trials. Before each miniblock, participants were instructed to press a button on a handheld button box for faces that matched the Go condition of the miniblock, and to withhold pressing the button for faces that matched the No-Go condition of the miniblock. Those four miniblocks were presented in counterbalanced orders across the six functional runs (Fig. 1*A*), and two scan run orders were used (counterbalanced across subjects).

In each trial, a fixation cross appeared for 500 ms, followed by a face image that was either a target (Go) or nontarget (No-Go), which was presented for 500 ms. Then, a 2750–7000 ms intertrial interval followed (sampled from an exponential distribution). The AGNG task totaled 80 trials/run ($n = 480$ trials total across the task) and took ~40 min to complete.

Face stimuli. Emotional faces (happy, neutral, and fearful) consisted of 12 identities (half female) selected from the Macbrain Face Stimulus Set (http://www.macbrain.org/resources.htm). Faces were cropped to remove hair and neck, and matched for average luminance and RMS contrast. Emotional faces were presented at 13° × 13° using PsychoPy (Peirce, 2007). The full list of emotional face stimuli, example stimuli, and stimulus presentation scripts used in this study is available online at https://osf.io/rqa8w/.

AGNG metrics and behavioral analyses. As dependent measures, we examined task accuracy, as well as two indices of emotion-driven influence on task behavior (i.e., "affect-to-motor spillover"). Emotional valence typically biases behavioral action in a valence congruent manner, whereby appetitive stimuli (e.g., happy faces) facilitate approach behavior (Go responses, as reflected by shortened reaction times), whereas aversive stimuli (e.g., fearful faces) typically facilitate avoidance (increasing accuracy in No-Go trials). Therefore, we computed two difference scores reflecting the magnitude of affect-to-motor spillover; in Go trials, the reaction time difference between Go Fear and Go Happy trials (Fear – Happy RT); and for No-Go trials, the accuracy difference score between No-Go Fear and No-Go Happy trials (No-Go Fear – Happy Accuracy). We examined whether RT and accuracy were modulated by emotional valence using the lme4 package (Bates et al., 2015), and anova and emmeans (https://github.com/rvlenth/emmeans) functions in R.

Functional MRI methods

Image acquisition

Neuroimaging data were acquired in the UC Berkeley Henry H. Wheeler, Jr. Brain Imaging Center with a Siemens TIM/Trio 3T MRI scanner with a 32-channel RF (radio frequency) head coil. Whole-brain Blood Oxygenation Level-Dependent (BOLD) fMRI data were obtained using a T2*-weighted 2× accelerated multiband echoplanar imaging sequence (52 axial slices, 2.5 mm^3 isotropic voxels; 84 × 84 matrix, TR = 2000 ms; TE = 30.2 ms; flip angle = 80°; 222 image volumes/run). High-resolution T1-weighted MPRAGE gradient-echo sequence images were collected at the end of the session for spatial normalization (176 × 256 × 256 matrix of 1 mm^3 isotropic voxels; TR = 2300 ms; TE = 2.98 ms; flip angle = 9°).

fMRI data preprocessing

Functional neuroimaging data were preprocessed using FEAT (Smith et al., 2004; Jenkinson et al., 2012) implemented in FSL version 6.0.1. Preprocessing steps included removal of the first four functional volumes, high-pass filtering with a 90 s cutoff, FILM correction for autocorrelation in the BOLD signal, slice-time correction, motion correction using MCFLIRT, and creation of a confound matrix of points of framewise displacement changes of >0.5 mm to be used as regressors of noninterest in the analyses to control for movement-confounded activation. Data were smoothed with using a 3 mm full-width at half-maximum Gaussian spatial filter. Functional images were coregistered to a high-resolution (T1-weighted) anatomic image using a linear rigid body (6-DOF) transform (while maintaining native functional resolution; i.e., 2.5 mm^3 isotropic).

Regions of interest

Subcortical. The basolateral amygdala region of interest (ROI) was defined using the CITI atlas basolateral nuclear group definition (i.e., lateral, basolateral and basomedial/accessory basal nuclei) by Tyszka and Pauli (2016) thresholded at 50% and registered from MNI to participants' structural space using FNIRT (10 mm warp resolution) while maintaining native resolution (2.5 mm^3 isotropic).

Cortical. Prefrontal ROIs [FPl, mid-LPFC (BA9–46), BA25/subgenual ACC, and BA32] were obtained from the Oxford PFC Consensus Atlas (http://lennartverhagen.com/; Sallet et al., 2013; Neubert et al., 2014), thresholded at 25% and registered to participants' native surface space using Freesurfer (Reuter et al., 2012). Vertex coordinates in each of these ROIs were transformed into the native anatomic (volumetric) space, and ROI masks in volumetric space were constructed by

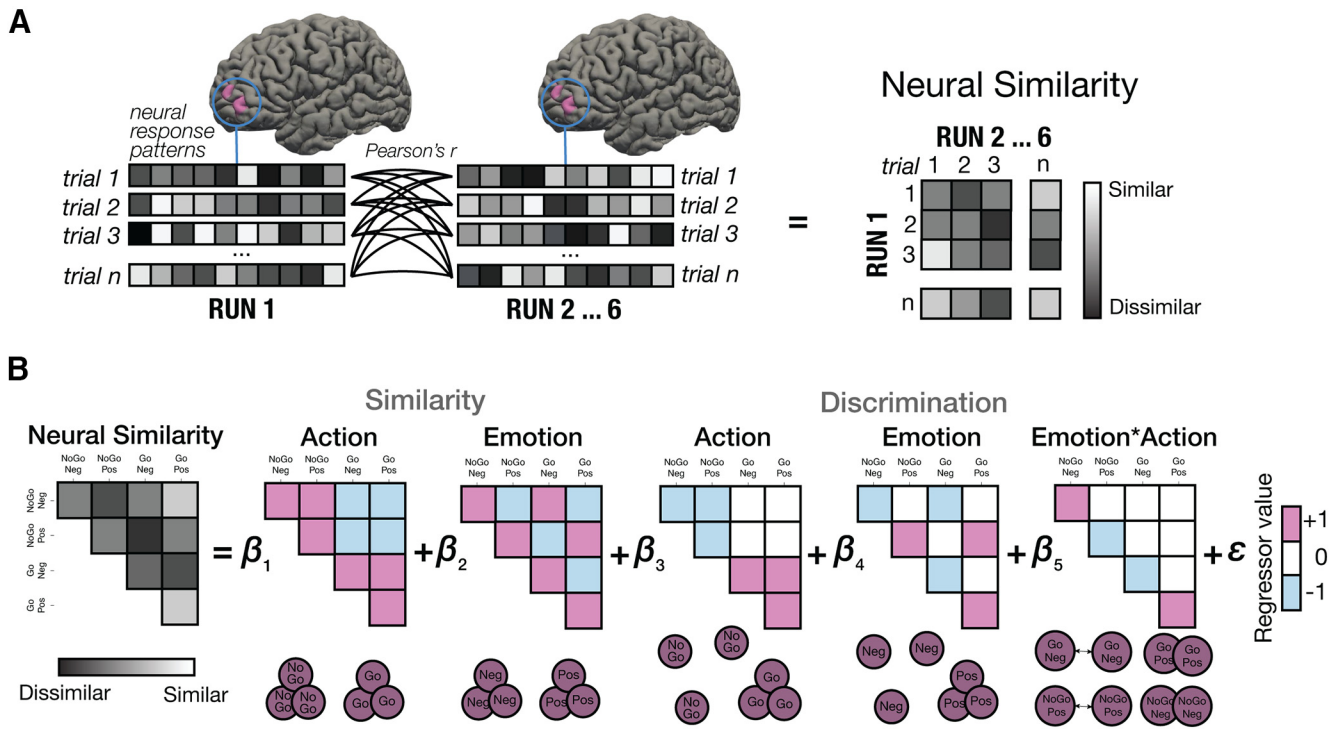

Figure 2. Pattern similarity analysis strategy. ***A***, Neural representational similarity matrices were obtained for each ROI by computing the correlation of multivoxel activity patterns across all trials of each condition obtained from independent scans (i.e., between-runs pattern similarity analysis). Each box denotes a voxel in the ROI, and each row denotes a trial. ***B***, Next, we used condition-specific template matrices to test whether neural similarity matrices were explained by action goal, emotional valence, and/or their interaction (conjunctive emotion * action goal representation). Template matrices tested differential representational distances by condition (discrimination matrices) as well as equivalent representational distances across different conditions (similarity matrices). Lower circles depict the representational structure captured by each regressor.

projecting half the distance of the cortical thickness at each vertex, requiring that a functional voxel be filled at least 50% by the label, and labeling the intersected voxels.

Regarding the rationale for the selection of our anatomical ROIs, we focused on BA9–46 dorsal (BA9–46d) + BA9–46 ventral (9–46v) because this mid-LPFC region, located in the middle frontal gyrus, has been shown to be a critical site of convergence of information relevant for cognitive control (Nee and D'Esposito, 2016). For the ventromedial PFC ROIs, we focused on BA25 and BA32 because both of these regions are known to be interconnected with the basolateral amygdala and frontopolar cortex in the nonhuman primate (Barbas and Pandya, 1989; Medalla and Barbas, 2010; Joyce and Barbas, 2018).

Statistical analysis

fMRI data modeling

For multivariate analyses (pattern similarity and classifier analyses), we obtained voxel-wise and trial-wise BOLD activation parameters estimates using the Least-Squares All general linear model (GLM) approach (Mumford et al., 2012) and FEAT modeling in FSL (Jenkinson et al., 2012). Single trials were modeled using a canonical hemodynamic response function (Double γ). Only correct trials were included in the analysis reported here (error trials were included in the model as a nuisance regressor). This amounted to up to 480 trials per participant (mean error = 5.783%, SD = 4.143%). In addition to single-trial and error-trial regressors, we modeled the 8 s instruction epoch using a canonical hemodynamic response function. Parameter estimates extracted from each ROI were regularized with multivariate noise normalization (Walther et al., 2016). To do so, we obtained an estimate of the noise covariance from the residuals of the GLMs from each ROI. This matrix was then regularized using the optimal shrinkage parameter, inverted, and multiplied by the vector of betas for each trial (Walther et al., 2016; Ballard et al., 2019). This approach removes nuisance correlations between voxels that arise because of physiological and instrument noise.

Pattern similarity analysis

We used pattern similarity analysis to examine the structure of emotion and action goal representations in FPl and interconnected circuitry (Kriegeskorte and Kievit, 2013). Pattern similarity analysis tests whether the intertrial similarity structure of multivoxel activity patterns (i.e., the neural similarity matrix) is explained by experimental factors—in the current experiment, emotional valence, action goal, and their interaction—which are expressed as pattern similarity analysis template matrices (Fig. 2). To obtain the neural similarity matrix for each participant and ROI, we computed pairwise Pearson correlations between pairs of multivoxel patterns obtained from all trials except for trials from the same run (i.e., a between-runs correlation approach, which is akin to a leave-one-run-out cross validation approach for multivariate classification analyses, and minimizes inflated correlations due to data dependencies and temporal autocorrelation; Fig. 2*A*). Pearson's correlations are distance metrics that are invariant to scale changes in multivoxel patterns. This approach yielded a trial-wise neural similarity matrix for each participant and ROI.

Next, we fit a multiple regression model using condition-specific template matrices to test whether the similarity structure of multivoxel patterns in the neural similarity matrix of each ROI was modulated by emotional valence, action goal, and/or their interaction (Fig. 2*B*). Because the AGNG task captures the differential impact of emotion on action based on action-goal congruency (i.e., positive and negative emotion differentially modulate Go and No-Go responses), our primary set of model matrices tested for discriminative similarity structures across unique combinations of emotion and action goal levels. In other words, these *discriminative* model matrices assess whether representational distances across a high-dimensional space are differentially modulated by emotion type or action–goal type [e.g., whether the average representational distance among distinct positively valenced events (trials) differs from the distance among negatively valenced events in a given brain region, or whether the distance among No-Go patterns differed from that of Go patterns]. Critically, the interactive discriminative matrix of emotional valence and action goal regressors (hereafter referred to as the emotion * action regressor) captures the emotion–action congruency

phenomenon studied here: "Go Positive" and "No-Go Negative" representations (i.e., congruent emotion–action conditions) are modeled closer in a high-dimensional space compared with "No-Go Positive" and "Go Negative" representations (incongruent conditions). Thus, by using three orthogonal discrimination matrices, we simultaneously modeled the impact of emotional valence, goal, and their interaction (conjunction) on neural similarity matrices (Fig. 2*B*).

To control for similarities across trials attributable to shared emotional valence or action goal conditions, we also included similarity template matrices in our simultaneous regression model (Fig. 2*B*). Those similarity matrices, in contrast to the discrimination matrices, tested for within-condition intertrial similarity while assuming equivalent representational distances across conditions (e.g., equivalent average pattern distance for positively and negatively valenced trials, collapsing across Go/No-Go action goal conditions). We fit the neural similarity matrices to these five total template matrices using a multiple regression mixed-model framework, where subject was modeled as a random factor, and each unique template matrix was included in the subject error term. This allowed us to test whether FPl and interconnected amygdala and LPFC circuitry represented the interaction of emotional valence or action goal (i.e., conjunctive representations), versus whether it represented emotional valence and/or action goal dimensions (Positive vs Negative; Go vs No-Go) as independent of one other. Importantly, this approach also allowed us to examine interactive effects while controlling for potential motor confounds arising from the Go versus No-Go conditions, given that the similarity patterns of Go and No-Go are entered simultaneously in the same regression model.

Multivariate pattern analysis

We used multivariate pattern analysis (MVPA) to examine whether emotional valence (Positive vs Negative) and action goal (Go vs No-Go) were linearly decodable in FPl and interconnected circuitry. MVPA used multivariate-noise normalized single-trial betas, as described above, and was implemented with Nilearn (Abraham et al., 2014). For each subject and ROI, we used a multivariate logistic regression model (l2 penalty; $C = 1$) to iteratively train the classifier on *z*-scored data. We assessed classifier performance using a leave-one-run-out cross-validation scheme. Classification performance was evaluated using the area under the curve (AUC; i.e., where 0.5 is chance performance). We examined whether the logistic classifier could distinguish emotional valence classes (Positive vs Negative) as well as action goal (Go vs No-Go). We used the Nilearn parameter (class_weight='balanced') to automatically adjust weights according to class frequencies in the input data (which is important for classification of Go vs No-Go classes). To examine whether classification accuracy differed from chance, we combined run-wise classifier AUCs (−0.5) across subjects using a mixed-model approach, where subject and run were entered as random factors, and tested whether the intercept differed significantly from 0.

MVPA–behavior correlations

We tested the behavioral relevance of the strength of classifier evidence for emotional valence and action goal in FPl using both an intraindividual analysis and an across-subjects analysis. For the intraindividual analysis, we regressed run-wise estimates of classifier AUC for emotional valence and action goal on run-wise estimates of task accuracy and affect-to-motor spillover [i.e., emotion-based difference scores in RT (Go trials) and accuracy (No-Go trials)]. For analyses across subjects, we examined the Spearman's ρ coefficient of the association among classifier AUC, task accuracy, and affect-to-motor spillover indices. The difference of dependent correlation coefficients was tested using the cocor package in R (http://comparingcorrelations.org/).

Functional connectivity analysis

To examine the putative origins of emotional valence information arriving in FPl, we used psychophysiological interaction (PPI) analysis (O'Reilly et al., 2012). To do so, we first extracted the mean time series from FPl and BLA ROIs. We then ran a separate FEAT analysis that included emotional valence task regressors, the demeaned time course of the ROI seed, as well as the interaction between this time course and the regressors encoding positive and negative emotional stimuli. The betas (parameter estimates) obtained from the interaction contrast were extracted for each subject, functional run, and ROI. As extreme outliers were observed, run-wise betas that exceeded ±4 SDs from the mean (across subjects) were excluded before analyses. To test whether BLA–BA25 significantly coupled during the AGNG task, betas obtained were entered into a mixed-effects model (where subject and run were entered as random factors) to test whether the intercept differed significantly from zero. Finally, run-wise variation in BA25–FPl functional coupling (PPI betas) were used to predict emotional valence classifier accuracy in FPl (with subject and run entered as random factors).

Results

Behavioral analysis: emotion biases action goal as evidenced by reaction time and accuracy metrics

We first verified whether emotion biased the execution of action goals in the AGNG task (Fig. 1*B*,*C*). As predicted, we found that emotion–action congruency influenced behavior as indexed by both reaction time and accuracy measures: in Go trials, Go target happy faces reduced reaction times relative to Go fearful faces ($F_{(1,36)} = 66.242$, $p < 0.001$, $d = 1.338$), which is consistent with appetitive states facilitating one's behavioral approach in the goal-congruent Go condition (Fig. 1*B*). In contrast, fearful faces increased accuracy in No-Go trials compared with happy faces ($z = 2.024$; $p = 0.043$, $d = 0.33$), which is consistent with aversive states facilitating avoidance in the goal-congruent No-Go condition (Fig. 1*C*). The impact of emotion on AGNG accuracy was specific to No-Go trials, as indicated by the interaction of emotional valence and action goal ($F_{(1,36)} = 4.104$, $p = 0.05$). In sum, emotional valence facilitated or hindered action depending on the congruency of emotion and action goal, with positive emotional states facilitating approach (Go) and negative emotional states facilitating avoidance (No-Go) responses, as evidenced by reaction time and accuracy metrics, respectively.

Pattern similarity analysis: conjunctive representations of emotion and action goal in FPl and amygdala

Next, we tested whether emotion–action congruency modulated the structure of neural representations in FPl and interconnected circuitry. In other words, do emotional states change the representation of action goals? If so, this implies that a region carries a conjunctive (i.e., integrated) representation of emotion and goal. To answer this question, we used pattern similarity analysis. Pattern similarity analysis tests whether the intertrial similarity structure of multivoxel activity patterns (i.e., the neural similarity matrix) is explained by experimental factors—in this case, emotional valence, action goal, and, critically, their interaction (Fig. 2).

To that end, we first computed neural similarity matrices for each ROI (Fig. 2*A*). Next, we used condition-specific template matrices to test whether neural similarity matrices were explained by emotional valence, action goal, and/or their interaction (i.e., conjunctive emotion * action representations). To account for the distinct ways in which emotion and action may be represented in the brain, we used the following two sets of template matrices in our model. (1) One set tested for differential representational distances between different emotion and action goal conditions, as well as their interaction (emotion * action). These comprised our primary regressors of interest (we refer to these matrices as condition discrimination matrices). (2) We also included orthogonal template matrices that tested for within-condition similarity (equivalency) in representational distances across emotion

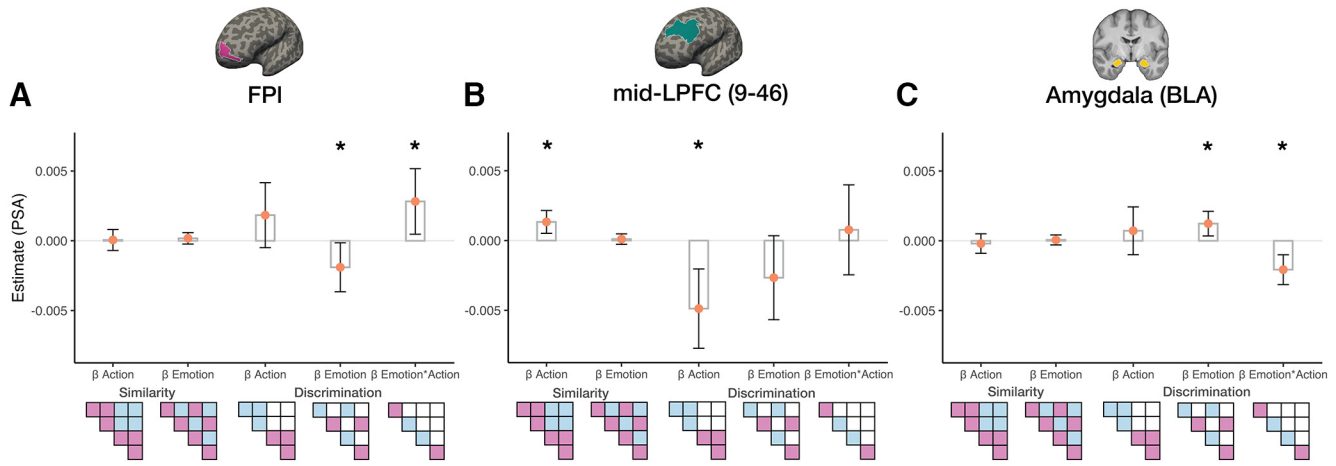

Figure 3. Pattern similarity analysis. ***A–C***, A simultaneous regression analysis of orthogonal template matrices on neural similarity matrices using a mixed-effects model revealed that FPl (***A***) and BLA (***C***) show evidence of conjunctive emotion * action goal representations, whereas mid-LPFC shows evidence of action goal representations unaltered by emotional valence (***B***). The *y*-axis shows the fixed-effects regression weights from the mixed-model regression for each ROI. While emotion and action goal are integrated into a higher-order representation in both FPl and BLA, their representational geometries are flipped in sign. Specifically, emotion–action congruent conditions (e.g., Go Positive or No-Go Negative) are represented closer in a high-dimensional space in FPl relative to incongruent conditions (e.g., Go Negative or No-Go Positive; ***A***), whereas the opposite was observed in the amygdala, wherein emotion–action incongruent trials were represented more similarly than congruent trials (***C***). The strength of emotion–action conjunctive coding differed significantly across the three ROIs, being significantly stronger in FPl and amygdala compared with mid-LPFC, p values < 0.0001. *$p < 0.05$.

and action goal conditions (similarity matrices; Fig. 2*B*; see Materials and Methods for additional details). We fit these template matrices on the neural similarity matrix using a simultaneous multiple regression mixed-model approach, with subject as a random intercept, and condition (each template matrix model) included in the subject error term. This approach tests whether FPl and interconnected circuitry have integrated or independent emotion/action goal representations.

We found evidence of conjunctive representations of emotion and action goal in FPl, as demonstrated by the significant fit of the interaction emotion * action regressor [$B = 0.003$ (SE = 0.001), $t = 2.354$, $p = 0.024$, p_{FDR} (false discovery rate adjusted) = 0.036; Fig. 3*A*]. This result indicates that trials were represented more similarly in a high-multidimensional space when emotion and action goal were congruent (Go Positive and No-Go Negative) than incongruent. Thus, emotional context sculpted action goal representations in FPl, suggesting that FPl integrates internal states and goal representations. In contrast, in mid-LPFC, the representation of action goals was unaltered by emotional valence (emotion * action interaction regressor, $p > 0.64$; Fig. 3*B*). Only action goal significantly explained the neural similarity structure observed in mid-LPFC [action goal similarity: $B = 0.001$ (SE = 0.0004), $t = 3.194$, $p < 0.003$, $p_{FDR} < 0.011$; action goal discrimination: $B = -0.005$ (SE = 0.001), $t = -3.364$, $p < 0.002$, $p_{FDR} < 0.009$]. Conjunctive representations of emotional valence and action goal were significantly stronger in FPl than in mid-LPFC ($z = 5.071$, $p < 0.0001$), suggesting regional specificity in conjunctive emotion–action representations in LPFC circuitry. We note that the emotional valence discrimination regressor also explained significant variance in the similarity structure of FPl [$B = -0.002$ (SE = 0.001), $t = -2.124$, $p = 0.041$, $p_{FDR} = 0.048$]. However, caution is warranted when interpreting simple effects from lower-order terms in a model that includes an interaction (accordingly, the simple effect of emotional valence in FPl is nonsignificant when the interaction of emotion * action is excluded from the model ($p > 0.79$), suggesting that the representational geometry of emotional valence in FPl may depend on goal state).

Next, we examined the representational structure of emotion and action goal in the basolateral amygdala. We found that the basolateral amygdala, like FPl, also expressed conjunctive emotion–action goal representations [$B = -0.002$ (SE = 0.001), $t = -3.797$, $p < 0.001$, $p_{FDR} < 0.006$; Fig. 3*C*]. However, the conjunctive emotion * action goal coding in the amygdala differed markedly from that in FPl: in the amygdala, emotion–action incongruent trials were represented closer together in a high-multidimensional space relative to emotion–action congruent trials. Conjunctive emotion * action goal representations were stronger in the amygdala than in mid-LPFC ($z = -10.400$, $p < 0.0001$). As expected, given their opposite signs, conjunctive coding in FPl significantly differed from that observed in the amygdala ($z = 6.312$, $p < 0.0001$). We note that the emotional valence discrimination regressor also explained significant variance in amygdalar similarity structure [$B = 0.001$ (SE = 0.0004,) $t = 2.742$, $p < 0.009$, $p_{FDR} = 0.026$], which, as mentioned above, should be interpreted with caution given that the emotion * action interaction is significant (as was the case with FPl, the simple effect of emotional valence in the amygdala was not observed when the emotion * action regressor was removed from the model, $p > 0.46$). In summary, emotional valence shaped the representation of action goal in the FPl–amygdala circuitry, with regionally specific representational geometries.

We next tested whether the strength of conjunctive emotion * action goal representations correlated with task performance. We hypothesized that the conjunctive representational structure observed in FPl, in which emotion-congruent trials are represented more similarly, is behaviorally advantageous. We found that conjunctive coding in FPl was associated with higher task accuracy (Spearman's $\rho = 0.33$, $p = 0.048$, $p_{FDR} = 0.048$; Fig. 4). This relationship was driven by the similarity among congruent emotion–action trials ($\rho = 0.42$, $p = 0.01$, $p_{FDR} = 0.026$; as opposed to dissimilarity among incongruent trials: $\rho = -0.1$, $p > 0.5$). This association was not observed in the basolateral amygdala ($\rho = 0.12$, $p > 0.47$); although note that FPl versus amygdala correlations were not significantly different ($p > 0.1$). These results suggest that conjunctive emotion–action representations in FPl support adaptive action selection during emotional processing.

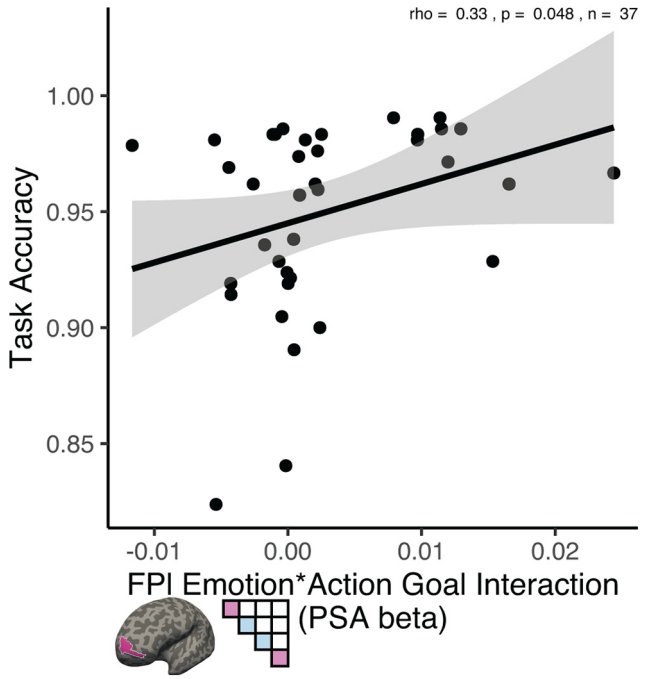

Figure 4. Association between task accuracy and the magnitude of conjunctive representation of emotion and action goal in FPl [as indicated by the β-coefficient of the emotion * action goal interaction in the pattern similarity analysis (PSA) regression model shown in Fig. 3*A*] across participants.

The behavioral relevance of action goal and emotional valence representations in FPl

High-dimensional (conjunctive) cognitive control representations are useful because they facilitate context-appropriate behavior, but fully conjunctive representations of, for example, emotional valence and action goal, do not necessarily permit a downstream region to linearly decode both factors independently of one another. It may be behaviorally advantageous for FPl to maintain linearly discriminable representations of valence and action goal in addition to their conjunction as to render the neural population more expressive (Badre et al., 2021). Whether a downstream region implementing linear decoding can read out this information depends on the geometry of the neural representation (Barak et al., 2013; Fusi et al., 2016; Badre et al., 2021). Therefore, we examined whether emotional valence and action goal in FPl and interconnected circuitry were linearly separable. We used a leave-one-run out cross validation approach, and combined run-level logistic classifier AUCs across subjects using mixed-models, to evaluate the discriminability of representations of emotional valence and action goal.

In FPl, we found evidence of linearly separable representations of both emotional valence and action goal [emotional valence classifier accuracy: mean = 51.6%, $B = 0.016$ (SE = 0.007), $t = 2.223$, $p = 0.032$, $p_{FDR} = 0.041$; action goal classifier accuracy: mean = 51.99%, $B = 0.0198$ (SE = 0.007), $t = 2.84$, $p = 0.015$, $p_{FDR} = 0.034$, respectively; Fig. 5*A*]. In mid-LPFC, classifier evidence was above chance for action goal [mean = 57.11%, $B = 0.07$ (SE = 0.012), $t = 5.737$, $p < 0.001$, $p_{FDR} < 0.006$] but not emotional valence [mean = 50.48%, $B = 0.005$ (SE = 0.007), $t = 0.642$, $p > 0.53$; Fig. 5*B*]. In the basolateral amygdala, neither emotional valence nor action goal categories were discriminable (mean = 50.66%, $p > 0.39$; and mean = 50.01%, $p > 0.99$, respectively; Fig. 5*C*). The strength of classifier evidence for action goal differed across regions ($F = 49.361$, $p < 0.001$), such that action goal representations in both mid-LPFC and in FPl were significantly stronger than in the basolateral amygdala ($t = -9.613$, $p < 0.0001$; and $t = -2.679$, $p = 0.008$, respectively), and greater in mid-LPFC than in FPl ($t = 6.934$, $p < 0.0001$). However, the strength of classifier evidence for emotional valence representation, while only significant in FPl, did not differ significantly across regions (p values > 0.134).

Given that emotional valence and action goal representations in FPl were linearly separable, we next examined whether they were associated with task performance and emotion-driven behavior in the AGNG task. Stronger action goal representations in FPls were associated with greater task accuracy within individuals and across runs [mixed-model $B = 0.077$ (SE = 0.033), $t = 2.322$, $p = 0.021$, $p_{FDR} = 0.034$; Fig. 6*A*]. Across individuals, and collapsing across runs, this association was also positive, albeit nonsignificant ($\rho = 0.29$, $p = 0.08$; Fig. 6*B*). Moreover, stronger action goal representations in FPl were associated with less affect-to-motor spillover across participants, as indexed by slower reaction times in negatively valenced Go trials relative to positively valenced Go trials ($\rho = -0.38$, $p = 0.02$, $p_{FDR} = 0.034$; Fig. 6*C*). Conversely, stronger emotional valence representations in FPl correlated with increased affect-to-motor spillover in No-Go trials, as indexed by higher accuracy in negatively valenced No-Go relative to positively valenced No-Go trials ($\rho = 0.37$, $p = 0.02$, $p_{FDR} = 0.034$; Fig. 6*D*). In other words, emotion-driven action tendencies benefited goal-driven action in trials where emotional valence and goal-based action were congruent, as is the case whenever negative facial expressions were the No-Go cues. All other relationships between decoding and behavior were nonsignificant. These results suggest that high-fidelity action goal representations in FPl facilitate task performance and reduce the influence of emotion on behavior, whereas stronger emotion representations in FPl increase the influence of emotion on behavior. However, we note the caveat that action and emotion decoding were each only related to one of our two affect-to-motor spillover measures (Go RT and No-Go accuracy, respectively).

Medial prefrontal contributions to emotional valence representation in FPl

While emotional valence information was present in FPl and modulated action goal representations, it remains unclear how FPl gains access to this information. FPl access to internal states has been postulated to rely on projections from ventromedial PFC (vmPFC) regions (Badre and Nee, 2018). Specifically, two distinct vmPFC regions, BA25 and BA32, are interconnected with the basolateral amygdala and project to the frontopolar cortex in the nonhuman primate (Barbas and Pandya, 1989; Medalla and Barbas, 2010; Joyce and Barbas, 2018).

To probe whether vmPFC conveys emotional valence information to FPl, we tested whether the strength of emotional valence classifier evidence in FPl covaried between FPl and BA25 as well as between FPl and BA32. We found that the strength of emotional valence decoding in BA25 predicted emotional valence decoding in FPl [$B = 0.152$ (SE = 0.068), $t = 2.219$, $p = 0.0275$, $p_{FDR} = 0.038$; Fig. 7*A*; in contrast, emotional valence decoding in BA32 and FPl did not correlate, $p > 0.27$]. Of note, BA25 is thought to be the primary vmPFC target and source of amygdala projections (Ghashghaei et al., 2007). Task-dependent functional connectivity analysis (PPI) confirmed that BA25 functionally coupled with the basolateral amygdala during negative emotional processing trials [$B = 0.361$ (SE = 0.139), $t = 2.6$, $p < 0.001$, $p_{FDR} < 0.006$; Fig. 7*B*]. The PPI fit was nonsignificant

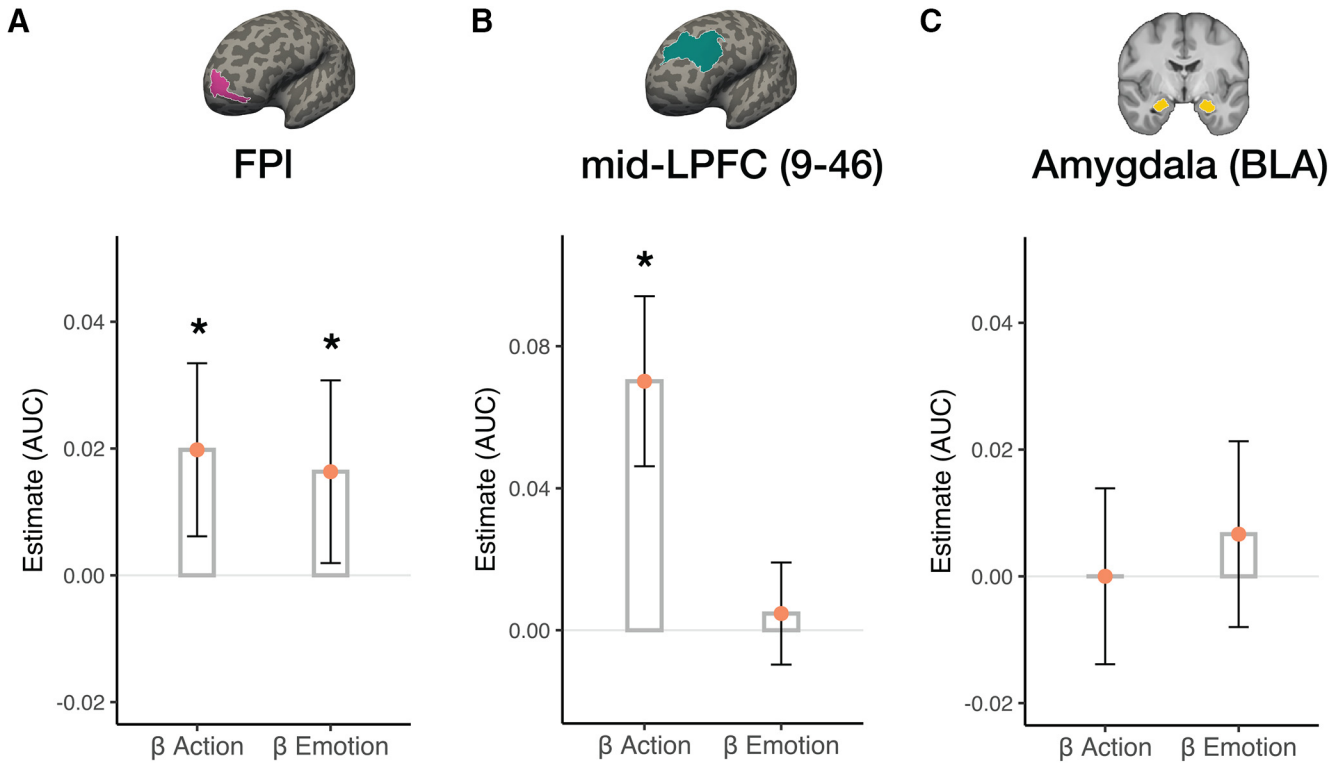

Figure 5. Decoding of emotional valence and action goal representations in FPl–amygdala circuitry. ***A–C***, Subject-wise and run-wise classifier AUCs for emotional valence and action goal were tested against zero using a mixed-effects model for each ROI; β-coefficients for each regression model are plotted for FPl (***A***), mid-LPFC (***B***), and BLA (***C***). *$p < 0.05$.

in BA32 during negative or positive emotional processing (p values > 0.69), or in BA25 during positive emotional processing ($p > 0.503$). Emotional valence classifier accuracy was above chance in BA25 [mean = 51.95%, $B = 0.02$ (SE = 0.009), $t = 2.195$, $p = 0.048$, $p_{FDR} = 0.048$], but not in BA32 [mean = 49.27%, $B = -0.007$ (SE = 0.008), $t = -0.974$, $p = 0.336$].

We next examined whether functional interactions between BA25 and FPl were associated with the encoding of emotional valence of FPl. We found that the magnitude of BA25–FPl coupling during negative emotional processing correlated with the strength of emotional valence classifier evidence in FPl [$B = 0.006$ (SE = 0.003), $t = 2.02$, $p = 0.045$, $p_{FDR} = 0.048$; Fig. 7*C*]. Collectively, these data suggest that BA25 function facilitates the flow of emotional valence information into FPl, which contextualizes goal representations based on variation on ongoing emotional states.

Discussion

Using pattern similarity analysis of fMRI data, we found that emotional context sculpted action goal representations in FPl: emotion and action goal were integrated in FPl into conjunctive representations. In contrast, in mid-LPFC, action goal representations were not modulated by emotion. In FPl, conjunctive emotion–action goal representations were modulated by emotion–action congruency. Moreover, the extent of these neural emotion–action congruency effects correlated with task accuracy. In FPl, but not in mid-LPFC or basolateral amygdala, action goal and emotional valence information were linearly separable, associated with task accuracy and with affect-to-motor spillover. Functional connectivity analyses revealed that BA25 (subgenual ACC) in the vmPFC served as the likely source of emotional valence information arriving in FPl. Collectively, these findings add to a growing literature pointing to a key role for FPl in the modulation of motivated action (Volman et al., 2011; Bramson et al., 2020; Kim et al., 2020). While prior work had demonstrated that FPl function plays an important role in the control of approach and avoidance behavioral tendencies (Volman et al., 2011; Koch et al., 2018; Bramson et al., 2020), the precise neural–representational mechanisms underlying the flexible use of goal-based signals and emotional context during cognitive control had not been previously specified.

Implications for theories of cognitive control

Conjunctive representations have been postulated to both increase behavioral flexibility and minimize interference when behavior depends on context (Badre et al., 2021). These features should be particularly relevant in emotionally provocative situations: during emotional processing, contextual emotion–goal integration is critical—otherwise, behavioral responses may become excessively emotion driven (e.g., guided by automatic action tendencies such as approach or withdrawal regardless of goals) or excessively goal driven, at the cost of failing to automatically incorporate important socioemotional cues in the environment (as is the case in psychopathy; Baskin-Sommers et al., 2016). Our finding that conjunctive emotion–action goal representations in FPl were associated with task performance supports the proposal that high-dimensional control representations are behaviorally advantageous (Fusi et al., 2016; Bernardi et al., 2020; Kikumoto and Mayr, 2020; Badre et al., 2021).

The utility of conjunctive representations depends partially on the extent to which important components comprising the conjunction can be read out by downstream circuitry (Fusi et al., 2016; Badre et al., 2021). Accordingly, we found that conjunctive representations of emotional valence and action rule in FPl were linearly separable. Moreover, the

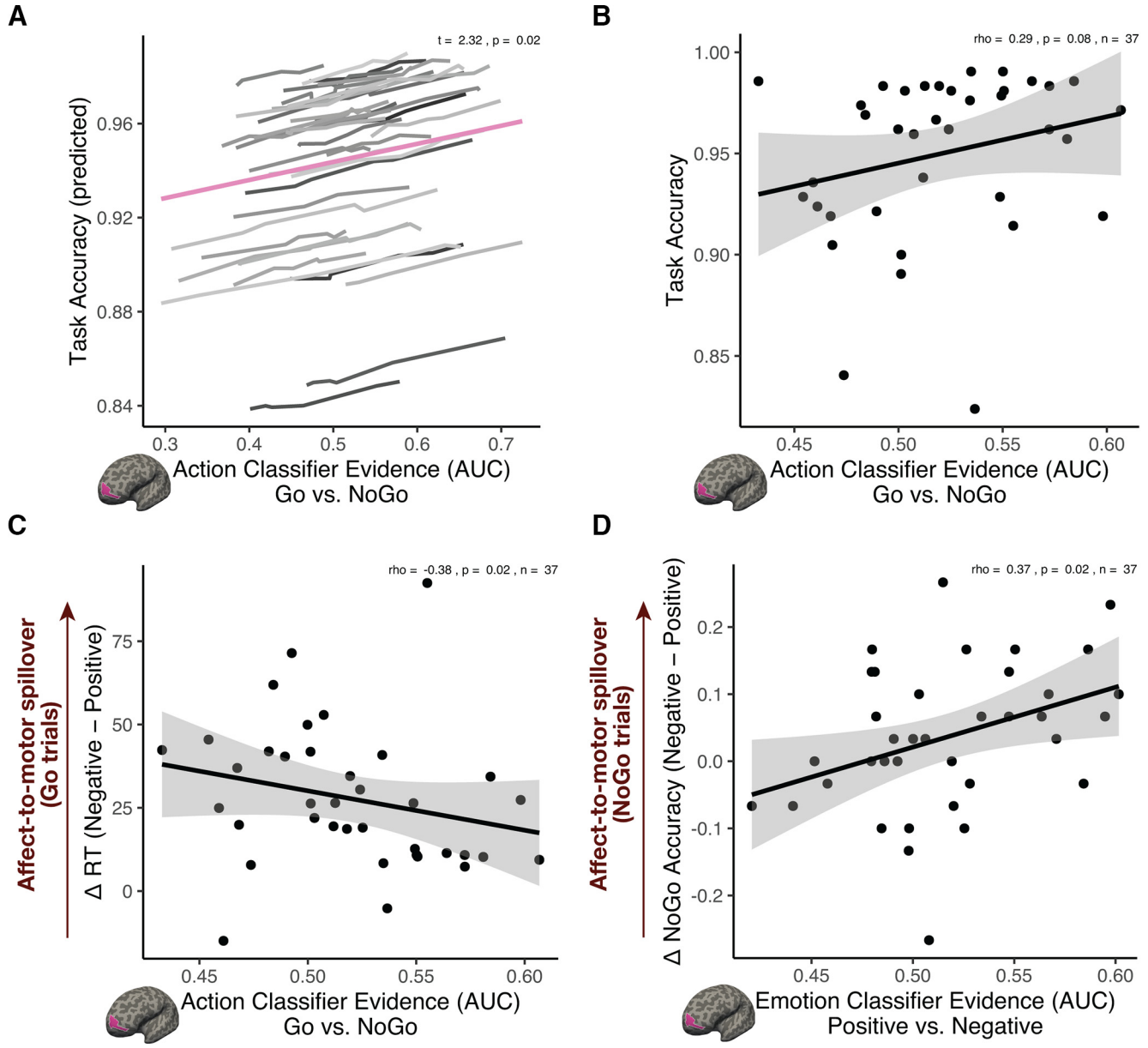

Figure 6. Association between behavior in the AGNG task and strength of action goal and emotional valence representations in FPl. ***A***, Stronger classifier evidence for action goal in FPl was associated with greater task performance within individuals, as evidenced by a mixed-effect model. ***B***, A similar trend was observed across subjects, wherein action goal classifier evidence in FPl tended to correlate positively with task performance in the AGNG task. ***C***, Stronger classifier evidence for action goal in FPl was inversely associated with affect-to-motor spillover in Go trials, as indicated by the faster reaction times in Go-positive relative to Go-negative trials. ***D***, Conversely, stronger classifier evidence for emotion in FPl correlated with greater affect-to-motor spillover in No-Go trials, as indicated by higher accuracy in No-Go-negative relative to No-Go-positive trials.

strength of action goal representations in FPl correlated with task performance and reduced affect-to-motor spillover, whereas the strength of emotional valence representations in FPl correlated with emotion-driven benefits in task accuracy (increased affect-to-motor spillover). Collectively, these data suggest that FPl representations guide emotional-context appropriate behavior, while supporting the ability to disentangle emotional context from rule-guided cues.

Implications for our understanding of prefrontal function in studies of emotion–cognition interactions

In models of emotion–cognition interactions, such as during the cognitive regulation of emotion, the LPFC is often postulated to subserve domain-general cognitive control in the form of goal-representation and maintenance (Braunstein et al., 2017; Kelley et al., 2018). However, that assertion has only rarely been tested. Moreover, signals associated with the regulation of emotional conflict or interference (e.g., the Stroop or the AGNG task) have often been found in medial, rather than lateral, PFC regions (Etkin et al., 2006; Egner et al., 2008; Braunstein et al., 2017). Precisely how medial and lateral PFC may work in concert during emotionally provocative situations remained unclear. Collectively, our data reaffirm the role of mid-LPFC for (action) goal representation in situations of emotion–action conflict while also highlighting a pathway through which medial prefrontal (BA25) emotional encoding may become integrated with current goals in FPl.

Prior work probing the function of PFC engagement in studies of emotion–cognition interactions often used a univariate approach and have occasionally produced conflicting

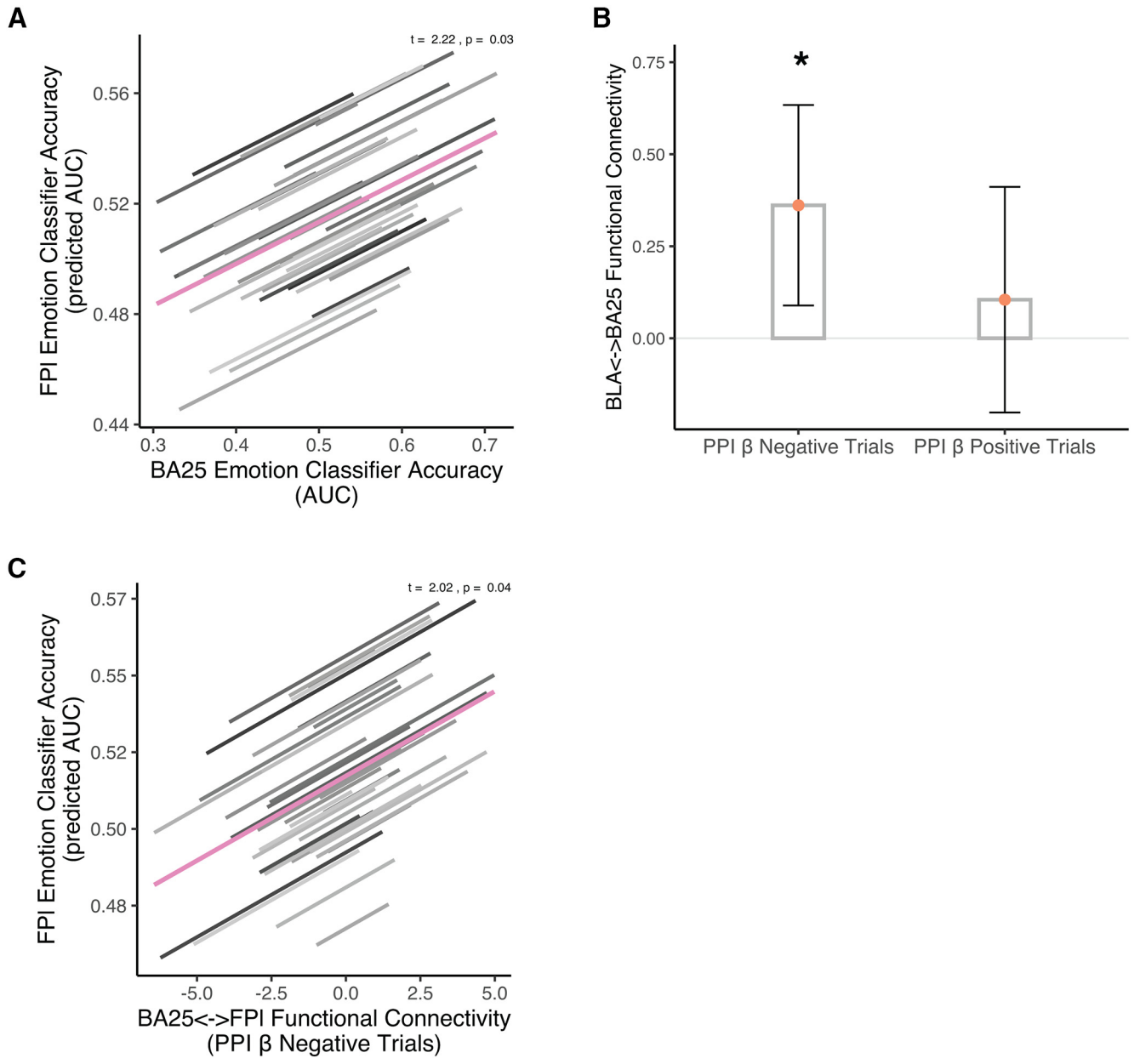

Figure 7. A pathway for emotional information flow from vmPFC (BA25) to FPI. ***A***, The strength of classifier evidence for emotional valence in BA25 (AUC) was a significant predictor of the strength of classifier evidence for emotional valence in FPI (AUC; run-wise mixed model). ***B***, A PPI analysis revealed that the BLA and BA25 functionally coupled during negative emotional processing trials, confirming well known dense anatomic projections between BLA and BA25 (Ghashghaei et al., 2007). ***C***, Further suggesting that BA25 may provide a key source of emotional valence information to FPI, the strength of BA25–FPI coupling during negative emotional processing (PPI) predicted the strength of classifier evidence for emotional valence in FPI (AUC).

findings. For instance, when examining the association between the engagement of LPFC regions and behavioral outcomes, prior work has found evidence for both performance-facilitatory effects (e.g., for overcoming distraction from emotional stimuli in working memory; Dolcos and McCarthy, 2006) as well as performance-hindering effects (e.g., where greater engagement of ventrolateral PFC was associated with more false alarms in an AGNG task; Somerville et al., 2011). Moving forward, we believe that a multivariate, representation-based approach may offer a promising way to reconcile these findings by allowing investigators to more directly interrogate not only which experimental variables (e.g., task structure vs emotional valence vs both) are represented by distinct prefrontal regions, but also to probe whether their relative strength of representation (as well as their integration) is associated with concomitant behavioral changes.

Of note, a large meta-analysis probing experimental factors driving engagement across a rich set of emotion–cognition interaction tasks (including emotional working memory, Stroop, and AGNG tasks) underscored that subgenual ACC (BA25) is particularly likely to be involved when emotional stimuli are task-relevant, consistent with present findings showing an emotional valence representational role for this region. Relatedly, the magnitude of subgenual ACC engagement in the AGNG task has been previously found to be beneficial for task performance in an adolescent sample (Hare et al., 2008). In contrast, mid-LPFC was found to be prominently involved when emotional stimuli are task irrelevant (also in agreement with our results, which highlight an action-goal,

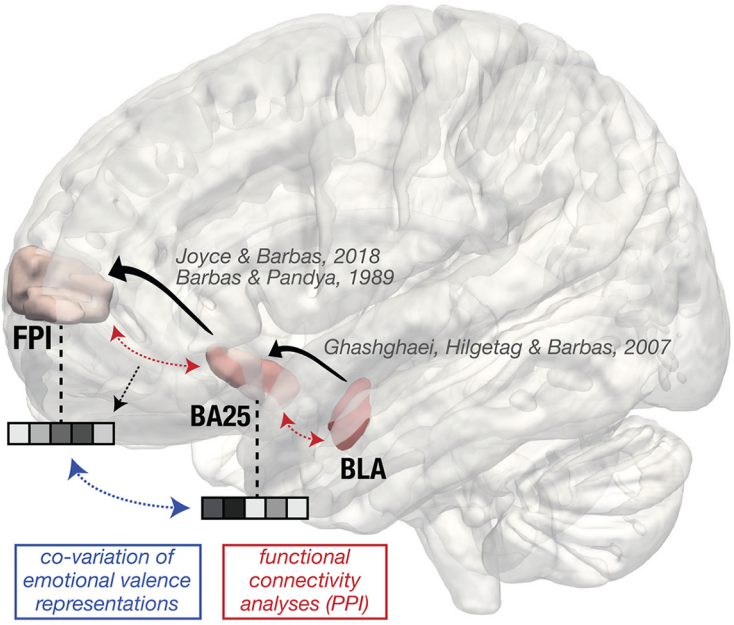

Figure 8. Summary of current results and extant neuroanatomical literature. Black arrows indicate neuroanatomical projections in the nonhuman primate, which are consistent with our findings from PPI and comultivariate decoding analyses. The significant covariation of classifier evidence for emotional valence found between BA25 and the FPl is highlighted in blue, and PPI results are indicated in red.

rather than a valence representational role for this region; Cromheeke and Mueller, 2014).

Conjunctive emotion–action representations in the basolateral amygdala

We also found evidence of conjunctive emotion–action representations in the basolateral amygdala. While we expected to find evidence of "pure" valence representation in this region given extant work in animal models (Tye, 2018), these results resonate with recent findings suggesting that amygdala neurons have mixed selectivity and represent contextual information. For instance, information about task sets, often observed in PFC neurons, is also decodable in single neurons in the nonhuman primate amygdala (Saez et al., 2015). Such abstract representations may provide important conceptual knowledge about when (and how) to respond to emotional events (Saez et al., 2015). Relatedly, amygdala intracranial event-related potentials during an AGNG task represent the interaction of emotional valence (negative vs neutral) and task rule (Go vs No-Go; Guex et al., 2020). Moreover, early work on the neural basis of the AGNG task suggested that the magnitude of univariate engagement of the amygdala in response to fearful targets can vary as a function of contextual background (being maximal when neutral faces—rather than happy faces—are nontargets; Hare et al., 2005). Together, these results demonstrate a broader, more goal-oriented and contextually sensitive role for amygdala neurons than its more commonly emphasized emotional valence and arousal encoding functions (Pignatelli and Beyeler, 2019).

In contrast to what we observed in FPl, in the amygdala, incongruent emotion–action trials were represented closer in a high-multidimensional space compared with congruent trials. Moreover, when controlling for the emotion * action interaction regressor, aversive (fearful face) trials were represented as more dissimilar in the basolateral amygdala compared with positive (happy face) trials (in FPl, positive trials were represented as more dissimilar than aversive trials). Greater pattern dissimilarity in amygdala multivoxel patterns in response to negatively valenced stimuli has been observed in response to unpleasant odors (Jin et al., 2015), which may support early discrimination of aversive stimuli. The functional significance of representational distances—multivoxel pattern similarity versus dissimilarity—is an ongoing area of study and varies by brain region (e.g., in hippocampus, pattern dissimilarity predicts better memory, in contrast to what is typically observed in neighboring brain regions such as perirhinal and parahippocampal cortices; LaRocque et al., 2013; Copara et al., 2014). It is possible that the observed dissimilarities for negative trials in the amygdala were due to competition of highly perceptually similar stimuli (i.e., negative and positive facial expressions of the same identity) and/or because of increased differentiation of specific face identities as they were repeated across the experiment; the design of the present study precluded disentangling these possibilities. Future work should further elucidate the temporal dynamics and behavioral significance of pattern dissimilarities in the amygdala and FPl.

Clarifying the neuroanatomy of emotional valence integration into action goals

Extant theories of the hierarchical organization of cognitive control in LPFC propose that the frontopolar cortex (rostrolateral PFC) is a node through which internal states, putatively originating from vmPFC, arrive in LPFC (Badre and Nee, 2018). Here, we examined this proposed pathway, and found converging evidence from functional connectivity and multivariate decoding analyses that a vmPFC region known to be densely interconnected with the amygdala and essential for emotion regulation, subgenual ACC (BA25), was the likely source of emotional signals arriving in FPl (Fig. 8). First, the strength of multivariate decoding of emotion in BA25 significantly predicted the strength of emotion decoding in FPl. Second, BA25 and basolateral amygdala significantly coupled during negative emotional processing, consistent with known neuroanatomical projections (Barbas and Pandya, 1989; Ghashghaei et al., 2007; Joyce and Barbas, 2018). Further, the extent of functional coupling between BA25 and FPl during negative emotional processing predicted the strength of the multivariate decoding of the emotional valence of FPl. These associations were not found in a neighboring vmPFC region, BA32, suggesting some degree of specificity of BA25–FPl interactions in this task. Collectively, these findings clarify the neuroanatomical pathway through which goal-based action may be potentiated or hindered by internal emotional signals arriving in LPFC, and how cognitive control is shaped by internal states. Moreover, these findings are consistent with recent work underscoring the importance of the amygdala ventrofugal pathway for the regulation of emotional action, and they deepen our understanding of the nodes in the (likely polysynaptic) circuitry linking amygdala and FPl function (Folloni et al., 2019; Bramson et al., 2020).

Implications for our understanding of LPFC organization, FPl function, and mental health

Emotional information comprises a critical source of contextual input that has been seldom considered in models of cognitive control in LPFC. This is despite the fact that LPFC lesions are known to predispose individuals to depression (Koenigs et al., 2008), LPFC TMS is an effective treatment for depression, particularly when its vmPFC projections are considered (Fox et al., 2012), and causal perturbations to LPFC via TMS impair automatic emotion regulation (Lapate et al., 2017).

In theories of the organization of cognitive control, FPl was once considered the top of a hierarchical gradient of goal abstraction, although recent work suggests that abstraction is distributed along various nodes in LPFC, and that mid-LPFC may be the apex of the LPFC cognitive control hierarchy (Nee and D'Esposito, 2016, 2017), consistent with our finding that it held the strongest magnitude of action goal representations among the brain regions examined here. Nonetheless, it is clear that the integrative function of FPl cuts across stimulus domains in the service of complex behavior, as it is reliably engaged in conditions that involve relational processing and temporally abstract considerations, including alternative courses of action or counterfactuals (Christoff and Gabrieli 2000; Boorman et al., 2009; Badre and Nee, 2018; Koch et al., 2018). Our study adds to this literature by highlighting an important instance of the integrative function of FPl, through which emotional states can shape long-term goals and behavioral control with consequences for emotion regulation. Accordingly, recent work has shown that the extent to which FPl responds to the congruency of emotion and action goal (approach vs avoid) predicts stress responsivity and susceptibility to post-traumatic stress disorder (Kaldewaij et al., 2019, 2021).

Limitations

The following limitations of the present study warrant caution and additional investigation. First, the AGNG task has a strong motor component that may obscure the unambiguous decoding of action goal (separate from motor action representations). While the pattern similarity analysis approach allowed us to explicitly control for motor confounds, the linear classifier analysis does not. Future work should use a task that matches movement demands across approach and avoidance conditions (Bramson et al., 2020). Second, action goals may engage different neural processes than other types of goals, such as those unfolding at longer time scales. Third, the associations reported here are inherently correlational. Future work using noninvasive brain stimulation will be critical for understanding the specific contributions of representations in FPl and LPFC for adaptive emotional behavior.

Conclusion

This study unveils integrated emotion–action representations in FPl, which are linearly decodable and correlate with cognitive control performance during emotional processing. Collectively, these findings provide a deeper understanding of how emotions flexibly shape goal representations, a process that goes awry in psychopathy, as well as of how acute emotional states may disrupt goal-based emotion regulation in mood and anxiety disorders.

References

Abraham A, Pedregosa F, Eickenberg M, Gervais P, Mueller A, Kossaifi J, Gramfort A, Thirion B, Varoquaux G (2014) Machine learning for neuroimaging with Scikit-Learn. Front Neuroinform 8:14.

Badre D, D'Esposito M (2009) Is the rostro-caudal axis of the frontal lobe hierarchical? Nat Rev Neurosci 10:659–669.

Badre D, Nee DE (2018) Frontal cortex and the hierarchical control of behavior. Trends Cogn Sci 22:170–188.

Badre D, Bhandari A, Keglovits H, Kikumoto A (2021) The dimensionality of neural representations for control. Curr Opin Behav Sci 38:20–28.

Ballard IC, Wagner AD, McClure SM (2019) Hippocampal pattern separation supports reinforcement learning. Nat Commun 10:1073.

Barak O, Rigotti M, Fusi S (2013) The sparseness of mixed selectivity neurons controls the generalization–discrimination trade-off. J Neurosci 33:3844–3856.

Barbas H, Pandya DN (1989) Architecture and intrinsic connections of the prefrontal cortex in the rhesus monkey. J Comp Neurol 286:353–375.

Baskin-Sommers A, Stuppy-Sullivan AM, Buckholtz JW (2016) Psychopathic individuals exhibit but do not avoid regret during counterfactual decision making. Proc Natl Acad Sci U S A 113:14438–14443.

Bates D, Mächler M, Bolker B, Walker S (2015) Fitting linear mixed-effects models using Lme4. J Stat Softw 67:1–48.

Bernardi S, Benna MK, Rigotti M, Munuera J, Fusi S, Daniel Salzman C (2020) The geometry of abstraction in the hippocampus and prefrontal cortex. Cell 183:954–967.e21.

Boorman ED, Behrens TEJ, Woolrich MW, Rushworth MFS (2009) How green is the grass on the other side? Frontopolar cortex and the evidence in favor of alternative courses of action. Neuron 62:733–743.

Bramson B, Folloni D, Verhagen L, Hartogsveld B, Mars RB, Toni I, Roelofs K (2020) Human lateral frontal pole contributes to control over emotional approach–avoidance actions. J Neurosci 40:2925–2934.

Braunstein LM, Gross JJ, Ochsner KN (2017) Explicit and implicit emotion regulation: a multi-level framework. Soc Cogn Affect Neurosci 12:1545–1557.

Christoff K, Gabrieli JDE (2000) The frontopolar cortex and human cognition: evidence for a rostrocaudal hierarchical organization within the human prefrontal cortex. Psychobiology 28:168–186.

Cole MW, Ito T, Braver TS (2016) The behavioral relevance of task information in human prefrontal cortex. Cereb Cortex 26:2497–2505.

Copara MS, Hassan AS, Kyle CT, Libby LA, Ranganath C, Ekstrom AD (2014) Complementary roles of human hippocampal subregions during retrieval of spatiotemporal context. J Neurosci 34:6834–6842.

Cromheeke S, Mueller SC (2014) Probing emotional influences on cognitive control: an ALE meta-analysis of cognition emotion interactions. Brain Struct Funct 219:995–1008.

Dolcos F, McCarthy G (2006) Brain systems mediating cognitive interference by emotional distraction. J Neurosci 26:2072–2079.

Egner T, Etkin A, Gale S, Hirsch J (2008) Dissociable neural systems resolve conflict from emotional versus nonemotional distracters. Cereb Cortex 18:1475–1484.

Etkin A, Egner T, Peraza DM, Kandel ER, Hirsch J (2006) Resolving emotional conflict: a role for the rostral anterior cingulate cortex in modulating activity in the amygdala. Neuron 51:871–882.

Folloni D, Sallet J, Khrapitchev AA, Sibson N, Verhagen L, Mars RB (2019) Dichotomous organization of amygdala/temporal-prefrontal bundles in both humans and monkeys. ELife 8:e47175.

Fox MD, Buckner RL, White MP, Greicius MD, Pascual-Leone A (2012) Efficacy of transcranial magnetic stimulation targets for depression is related to intrinsic functional connectivity with the subgenual cingulate. Biol Psychiatry 72:595–603.

Fusi S, Miller EK, Rigotti M (2016) Why neurons mix: high dimensionality for higher cognition. Curr Opin Neurobiol 37:66–74.

Ghashghaei HT, Hilgetag CC, Barbas H (2007) Sequence of information processing for emotions based on the anatomic dialogue between prefrontal cortex and amygdala. Neuroimage 34:905–923.

Guex R, Méndez-Bértolo C, Moratti S, Strange BA, Spinelli L, Murray RJ, Sander D, Seeck M, Vuilleumier P, Domínguez-Borràs J (2020) Temporal dynamics of amygdala response to emotion- and action-relevance. Sci Rep 10:11138.

Hare TA, Tottenham N, Davidson MC, Glover GH, Casey BJ (2005) Contributions of amygdala and striatal activity in emotion regulation. Biol Psychiatry 57:624–632.

Hare TA, Tottenham N, Galvan A, Voss HU, Glover GH, Casey BJ (2008) Biological substrates of emotional reactivity and regulation in adolescence during an emotional go-nogo task. Biol Psychiatry 63:927–934.

Jacobs B, Schall M, Prather M, Kapler E, Driscoll L, Baca S, Jacobs J, Ford K, Wainwright M, Treml M (2001) Regional dendritic and spine variation in human cerebral cortex: a quantitative Golgi study. Cereb Cortex 11:558–571.

Jenkinson M, Beckmann CF, Behrens TEJ, Woolrich MW, Smith SM (2012) FSL. Neuroimage 62:782–790.

Jin J, Zelano C, Gottfried JA, Mohanty A (2015) Human amygdala represents the complete spectrum of subjective valence. J Neurosci 35:15145–15156.

Joyce MKP, Barbas H (2018) Cortical connections position primate area 25 as a keystone for interoception, emotion, and memory. J Neurosci 38:1677–1698.

Kaldewaij R, Koch SBJ, Zhang W, Hashemi MM, Klumpers F, Roelofs K (2019) Frontal control over automatic emotional action tendencies predicts acute stress responsivity. Biol Psychiatry Cogn Neurosci Neuroimaging 4:975–983.

Kaldewaij R, Koch SBJ, Hashemi MM, Zhang W, Klumpers F, Roelofs K (2021) Anterior prefrontal brain activity during emotion control predicts resilience to post-traumatic stress symptoms. Nat Hum Behav 5:1055–1064.

Kamali A, Sair HI, Blitz AM, Riascos RF, Mirbagheri S, Keser Z, Hasan KM (2016) Revealing the ventral amygdalofugal pathway of the human limbic system using high spatial resolution diffusion tensor tractography. Brain Struct Funct 221:3561–3569.

Kelley NJ, Gallucci A, Riva P, Romero Lauro LJ, Schmeichel BJ (2018) Stimulating self-regulation: a review of non-invasive brain stimulation studies of goal-directed behavior. Front Behav Neurosci 12:337.

Kikumoto A, Mayr U (2020) Conjunctive representations that integrate stimuli, responses, and rules are critical for action selection. Proc Natl Acad Sci U S A 117:10603–10608.

Kim ML, Elliott AR, Knodt AR Hariri (2020) A connectome-wide functional signature of trait anger. BioRxiv 338863.

Koch SBJ, Rogier B, Mars I, Toni K Roelofs (2018) Emotional control, reappraised. Neurosci Biobehav Rev 95:528–534.

Koenigs M, Huey ED, Calamia M, Raymont V, Tranel D, Grafman J (2008) Distinct regions of prefrontal cortex mediate resistance and vulnerability to depression. J Neurosci 28:12341–12348.

Kriegeskorte N, Kievit RA (2013) Representational geometry: integrating cognition, computation, and the brain. Trends Cogn Sci 17:401–412.

Lapate RC, Samaha J, Rokers B, Hamzah H, Postle BR, Davidson RJ (2017) Inhibition of lateral prefrontal cortex produces emotionally biased first impressions: a transcranial magnetic stimulation and electroencephalography study. Psychol Sci 28:942–953.

LaRocque KF, Smith ME, Carr VA, Witthoft N, Grill-Spector K, Wagner AD (2013) Global similarity and pattern separation in the human medial temporal lobe predict subsequent memory. J Neurosci 33:5466–5474.

Medalla M, Barbas H (2010) Anterior cingulate synapses in prefrontal areas 10 and 46 suggest differential influence in cognitive control. J Neurosci 30:16068–16081.

Mumford JA, Turner BO, Gregory Ashby F, Poldrack RA (2012) Deconvolving BOLD activation in event-related designs for multivoxel pattern classification analyses. Neuroimage 59:2636–2643.

Nee DE, D'Esposito M (2016) The hierarchical organization of the lateral prefrontal cortex. Elife 5:e12112.

Nee DE, D'Esposito M (2017) Causal evidence for lateral prefrontal cortex dynamics supporting cognitive control. Elife 6:e28040.

Neubert F-X, Mars RB, Thomas AG, Sallet J, Rushworth MFS (2014) Comparison of human ventral frontal cortex areas for cognitive control and language with areas in monkey frontal cortex. Neuron 81:700–713.

O'Reilly JX, Woolrich MW, Behrens TEJ, Smith SM, Johansen-Berg H (2012) Tools of the trade: psychophysiological interactions and functional connectivity. Soc Cogn Affect Neurosci 7:604–609.

Peirce JW (2007) PsychoPy–Psychophysics software in Python. J Neurosci Methods 162:8–13.

Pignatelli M, Beyeler A (2019) Valence coding in amygdala circuits. Curr Opin Behav Sci 26:97–106.

Reuter M, Schmansky NJ, Diana Rosas H, Fischl B (2012) Within-subject template estimation for unbiased longitudinal image analysis. Neuroimage 61:1402–1418.

Saez A, Rigotti M, Ostojic S, Fusi S, Salzman CD (2015) Abstract context representations in primate amygdala and prefrontal cortex. Neuron 87:869–881.

Sallet J, Mars RB, Noonan MP, Neubert F-X, Jbabdi S, O'Reilly JX, Filippini N, Thomas AG, Rushworth MF (2013) The organization of dorsal frontal cortex in humans and macaques. J Neurosci 33:12255–12274.

Smith SM, Jenkinson M, Woolrich MW, Beckmann CF, Behrens TEJ, Johansen-Berg H, Bannister PR, De Luca M, Drobnjak I, Flitney DE, Niazy RK, Saunders J, Vickers J, Zhang Y, De Stefano N, Brady JM, Matthews PM (2004) Advances in functional and structural MR image analysis and implementation as FSL. NeuroImage 23 [Suppl 1]:S208–S219.

Somerville LH, Hare T, Casey BJ (2011) Frontostriatal maturation predicts cognitive control failure to appetitive cues in adolescents. J Cogn Neurosci 23:2123–2134.

Tottenham N, Hare TA, Casey BJ (2011) Behavioral assessment of emotion discrimination, emotion regulation, and cognitive control in childhood, adolescence, and adulthood. Front Psychol 2:39.

Tye KM (2018) Neural circuit motifs in valence processing. Neuron 100:436–452.

Tyszka JM, Pauli WM (2016) In vivo delineation of subdivisions of the human amygdaloid complex in a high-resolution group template. Hum Brain Mapp 37:3979–3998.

Volman I, Roelofs K, Koch S, Verhagen L, Toni I (2011) Anterior prefrontal cortex inhibition impairs control over social emotional actions. Curr Biol 21:1766–1770.

Walther A, Nili H, Ejaz N, Alink A, Kriegeskorte N, Diedrichsen J (2016) Reliability of dissimilarity measures for multi-voxel pattern analysis. NeuroImage 137:188–200.

Waskom ML, Kumaran D, Gordon AM, Rissman J, Wagner AD (2014) Frontoparietal representations of task context support the flexible control of goal-directed cognition. J Neurosci 34:10743–10755.

Zhuang Q, Xu L, Zhou F, Yao S, Zheng X, Zhou X, Li J, Xu X, Fu M, Li K, Vatansever D, Kendrick KM, Becker B (2021) Segregating domain-general from emotional context-specific inhibitory control systems—ventral striatum and orbitofrontal cortex serve as emotion-cognition integration hubs. Neuroimage 238:118269.